

A gut microbial metabolite of dietary polyphenols reverses obesity-driven hepatic steatosis

Lucas J. Osborn^{1,2,3}, Karlee Schultz^{1,2,4,†}, William Massey^{1,2,3,†}, Beckey DeLucia^{1,2}, Ibrahim Choucair^{1,2}, Venkateshwari Varadharajan^{1,2}, Kevin Fung^{1,2}, Anthony J. Horak III^{1,2}, Danny Orabi^{1,2,3,5}, Ina Nemet^{1,2}, Laura E. Nagy^{3,6}, Zeneng Wang^{1,2}, Daniela S. Allende⁷, Naseer Sangwan^{1,2}, Adeline M. Hajjar^{1,2}, Christine McDonald^{3,6}, Philip P. Ahern^{1,2,3}, Stanley L. Hazen^{1,2,8}, J. Mark Brown^{1,2,3,*}, Jan Claesen^{1,2,3,*}

Affiliations:

¹Department of Cardiovascular and Metabolic Sciences, Lerner Research Institute of the Cleveland Clinic; Cleveland, OH, USA.

²Center for Microbiome and Human Health, Lerner Research Institute of the Cleveland Clinic; Cleveland, OH, USA.

³Department of Molecular Medicine, Cleveland Clinic Lerner College of Medicine of Case Western Reserve University; Cleveland, Ohio, USA.

⁴College of Arts and Sciences, John Carroll University; University Heights, OH, USA.

⁵Department of General Surgery, Cleveland Clinic; Cleveland, OH, USA.

⁶Department of Inflammation and Immunity, Lerner Research Institute of the Cleveland Clinic; Cleveland, OH, USA.

⁷Robert J. Tomsich Pathology and Laboratory Medicine Institute of the Cleveland Clinic; Cleveland, OH, USA.

⁸Department of Cardiovascular Medicine, Heart Vascular and Thoracic Institute, Cleveland Clinic; Cleveland, OH, USA.

†Contributed equally to this work.

*Co-Corresponding Authors: Jan Claesen, Email: claesej@ccf.org and J. Mark Brown, Email: brownm5@ccf.org

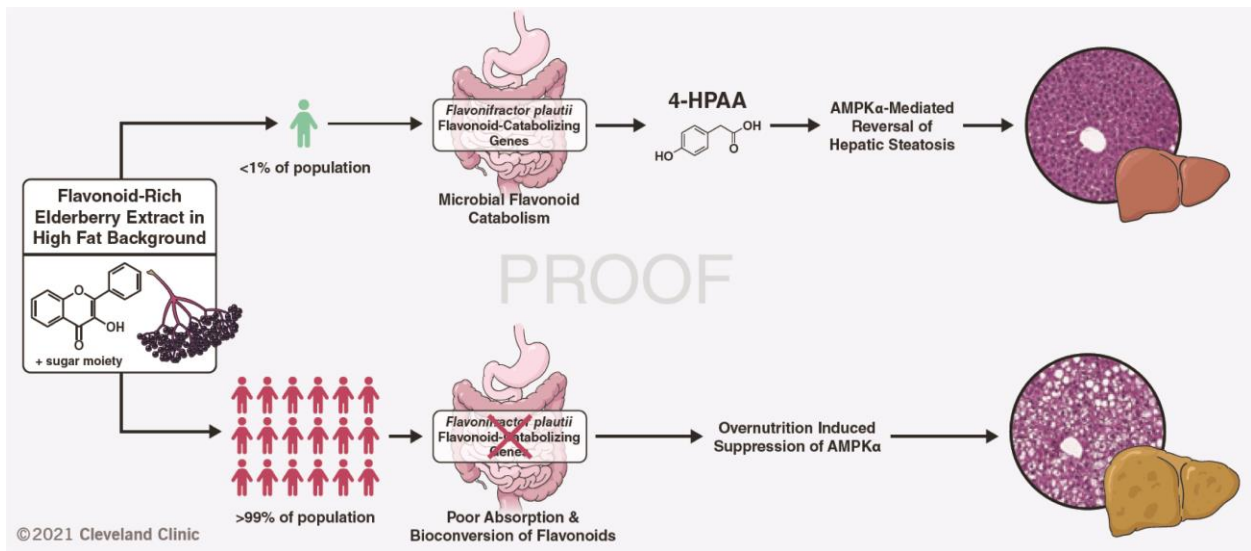
31
32
33
34
35
36
37
38
39
40
41
42
43
44
45
46
47

Abstract:

The molecular mechanisms by which dietary fruits and vegetables confer cardiometabolic benefits remain poorly understood. Historically, these beneficial properties have been attributed to the antioxidant activity of flavonoids. Here, we reveal that the host metabolic benefits associated with flavonoid consumption actually hinge on gut microbial metabolism. We show that a single gut microbial flavonoid catabolite is sufficient to reduce diet-induced cardiometabolic disease burden in mice. Dietary supplementation with elderberry extract attenuated obesity and continuous delivery of the catabolite 4-hydroxyphenylacetic acid was sufficient to reverse hepatic steatosis. Analysis of human gut metagenomes revealed that under one percent contains a flavonol catabolic pathway, underscoring the rarity of this process. Our study will impact the design of dietary and probiotic interventions to complement traditional cardiometabolic treatment strategies.

One-Sentence Summary: Select gut microbes can metabolize flavonoids from a fruit and vegetable diet to monophenolic acids, which improve fatty liver disease.

Graphical abstract:



48

49 **Main Text:**

50 A balanced diet is one of the most influential drivers of human health. This notion has become
51 increasingly important in our industrialized era, characterized by pervasive human metabolic
52 syndrome. More recently, diet has become appreciated as a focal determinant of gut microbial
53 community structure, function, and resilience where dietary choices are recognized to rapidly
54 alter the human gut microbiome (1). Moreover, diet-derived metabolites from the human gut
55 microbiota have been causally linked to cardiovascular and metabolic disease pathogenesis (2–
56 5). Consequently, microbial metabolites arising from specific dietary components, such as
57 trimethylamine (TMA), imidazole propionate and short-chain fatty acids (SCFAs), have gained
58 recognition as central mediators of human health and disease (2–6).

59
60 Flavonoids represent a key molecular component of plant-based diets. They have been attributed
61 antioxidant, antiobesogenic, and chemoprotective properties through the scavenging of free
62 radicals and activation of molecular effectors implicated in human disease (7). Dietary
63 flavonoids are largely glycosylated, limiting their absorption in the small intestine and thereby
64 their systemic distribution (7). Consequently, upon passing into the colon, flavonoids become a
65 substrate for gut microbial catabolism. Notable prior studies have highlighted that dietary
66 flavonoids attenuate diet-induced obesity in a microbe-dependent manner (8, 9). Several human
67 gut bacteria that are capable of breaking down flavonoid substrates through reduction and
68 subsequent cleavage of the central non-aromatic ring, followed by hydrolysis to yield
69 monophenolic acid degradation products have been isolated (10). The four types of bacterial
70 enzymes required in the flavone/flavonol catabolic pathway (flavone reductase (FLR), chalcone
71 isomerase (CHI), enoate reductase (EnoR), and phloretin hydrolase (PHY)) have been identified
72 and biochemically characterized (11–14). Together, these genes represent just one method by
73 which commensal gut bacteria metabolize host dietary inputs; additional homologous or non-
74 homologous pathways may remain undiscovered.

75
76 **Berry supplementation reduces the obesogenic effects of a high fat diet**

77 Since ingested flavonoids themselves have poor bioavailability, we hypothesized that their
78 microbial monophenolic acid catabolites are responsible for prior ascribed anti-obesogenic
79 properties (8, 9). To identify candidate catabolites, we used a comparative targeted metabolomics
80 analysis of mice that were supplemented three different flavonoid-rich berry extracts on a high
81 fat diet (HFD) background. For 16 weeks, we provided mice with ad libitum access to a high fat
82 control diet, or the same high fat diet base, supplemented with 1% w/w of either elderberry,
83 black currant, or aroniaberry extracts. Metabolic parameters including body weight, lean mass,
84 fat mass, and glucose homeostasis were tracked for the duration of the experiment. We observed
85 that elderberry extract-supplemented mice were markedly protected from HFD-induced obesity
86 (Fig. 1A-D, S1A, B). Moreover, elderberry extract-supplemented mice had more lean mass, less
87 fat mass, and were less hyperinsulinemic than HFD control mice 16 weeks after initiation of
88 differential diet treatments (Fig. 1E-G, S1C). Analysis of the cecal microbial composition by 16S
89 rRNA sequencing revealed that elderberry extract-supplemented mice had significantly more
90 diverse cecal microbial communities that clustered distinctly from the HFD control mice using

91 non-metric multidimensional scaling, and from the other berry extract-supplemented mice (Fig.
92 2A-C, S2A-I). Of note, *Lachnospiraceae* UCG-006 was only observed in the cecal communities
93 of berry-extract fed mice (light green in Fig. 2C, S2F). Moreover, other *Lachnospiraceae* clades
94 (*NK4A136* and *UCG-009*) were significantly more abundant in elderberry-extract fed mice when
95 compared to the HFD control group (Fig. 2C, S2G).

96
97 Provided that mice are likely to contain commensal gut microbes capable of catabolizing
98 flavonoids into monophenolic acids, we expected that these microbe-derived monophenolic acids
99 would be enriched in the portal plasma of berry extract-supplemented mice compared to the HFD
100 control. A targeted liquid chromatography-tandem mass spectrometry (LC-MS/MS) approach
101 revealed six known microbial flavonoid catabolites at detectable levels in portal plasma (15)
102 (Fig. 2D, S2J-N). Of the six metabolites, only 4-hydroxyphenylacetic acid (4-HPAA) and 4-
103 hydroxy-3-methoxybenzoic acid were significantly enriched in the portal plasma of elderberry-
104 supplemented mice compared to the HFD control (Fig. 2D, E, S2J). Between these two
105 metabolites, 4-HPAA had the largest fold difference in portal plasma concentration relative to
106 the HFD control (2.33 +/- 0.35, mean fold change +/- 95% confidence interval, n=9-10). In
107 addition, 4-HPAA correlated negatively with plasma insulin levels (Fig. S1C) ($R^2=0.206$,
108 $P=0.004$). Finally, plasma levels of 4-HPAA have been previously reported to associate
109 negatively with indices of obesity in a cohort of non-diabetic obese human subjects (16). Hence,
110 we selected 4-HPAA as our candidate molecule to test the hypothesis that a single microbial
111 flavonoid catabolite would be sufficient to abrogate key parameters of HFD-induced metabolic
112 disease.

113 114 **A single microbial flavonoid catabolite reverses hepatic steatosis**

115 To test whether the metabolically beneficial effects of elderberry supplementation could at least
116 in part be attributed to the microbial flavonoid catabolite 4-HPAA, we implanted subcutaneous
117 slow-release pellets delivering 4-HPAA (350 $\mu\text{g}/\text{day}$) into mice pre-fed a high fat diet to
118 establish obesity and compared them to obese control mice that received an implanted sham
119 scaffold for 6 weeks (Fig. 3A). This subcutaneous delivery method has been used previously to
120 study different microbial metabolites at a single-metabolite resolution (3). Its main advantage is
121 that the delivered molecule is independent of further modification by gut microbial metabolism,
122 a limitation of providing 4-HPAA in the diet or drinking water (3). After twenty-five days, we
123 surveyed global metabolism and energy substrate utilization using indirect calorimetry data to
124 compare the 4-HPAA and the scaffold-only control mice at isothermal 30 °C, room temperature
125 23 °C, and under cold challenge at 4 °C. We observed that 4-HPAA treated mice were more
126 prone to utilize carbohydrates as an energy source as measured by the respiratory exchange ratio
127 (RER) during the light cycle under cold exposure (Fig. S3A). At the time of sacrifice, the mRNA
128 expression of *Ucp1* (encoding a key regulator of non-shivering thermogenesis that mediates
129 oxygen consumption in cold conditions (17)) was increased in the metabolically active brown
130 adipose tissue of 4-HPAA treated mice (Fig. S2B). This suggests that 4-HPAA may modulate
131 metabolic flexibility during cold exposure.

132
133
134
135
136
137
138
139
140
141
142
143
144
145
146
147
148
149
150
151
152
153
154
155
156
157
158
159
160
161
162
163
164
165
166
167
168
169
170
171
172

After six weeks of continuous 4-HPAA exposure, modest changes in gross anthropometrics (Fig. 3B, C) were overshadowed by striking liver-specific effects of 4-HPAA. Consistent with our previous findings (18), 4-HPAA accumulates in the liver as it undergoes rapid first-pass hepatic metabolism (Fig. 3D). Remarkably, after just 6 weeks, subcutaneous 4-HPAA administration led to a marked reversal of hepatic steatosis when compared to control mice (Fig. 3E-G). We did not observe quantitative differences in the mild presentation of hepatocellular ballooning or lobular inflammation (Fig. 3H, I), yet 4-HPAA treated mice had lower plasma concentrations of the liver injury marker aspartate aminotransferase but not alanine aminotransferase (Fig. 3J, K).

To better understand the transcriptional foundations of the 4-HPAA mediated reduction of hepatic steatosis, we measured the mRNA expression of several genes implicated in lipid metabolism and inflammation in the liver (Fig. S3C). Here we observed a reduction in the fatty acid importer *Cd36*, the fatty acid desaturase *Scd1*, and the pro-inflammatory cytokine *Tnfa* in 4-HPAA treated mice with a concomitant increase in the master regulator of mitochondrial biogenesis, *Pgc1a* and *Lcn13*, a regulator of glucose and lipid metabolism (19–21). In addition, we measured the mRNA expression of lipid metabolism and inflammation-related genes in the gonadal white adipose tissue as it plays a central role in maintaining metabolic homeostasis (Fig. S3D). For 4-HPAA treated mice, we observed increased mRNA levels of lipoprotein lipase (*Lpl*), the adipocyte-specific isoform of peroxisome proliferator-activated receptor gamma (*Pparg2*, a master regulator of glucose homeostasis and lipid metabolism), as well as a reduction of the expression of macrophage-associated glycoprotein *Cd68*. Taken together, our data suggest that 4-HPAA confers a distinct metabolic benefit that is regulated in part by tissue-specific transcriptional reprogramming.

4-HPAA activates hepatic AMPK α signaling

We next set out to uncover the signaling cascade(s) that could be potentially linked to 4-HPAA induced transcriptional changes. We hypothesized that AMP-activated protein kinase (AMPK) signaling is upregulated in the livers of mice receiving subcutaneous 4-HPAA. Our reasoning was based on four premises (i) literature reports on the activation of AMPK by the structurally distinct monophenolic acids gallic acid, vanillic acid and caffeic acid (22–24), (ii) the observation that exogenously administered 4-HPAA accumulates in the liver, (iii) our observed transcriptional data that is consistent with AMPK activation (25), and (iv) physiologic hormone-driven activation of AMPK by adiponectin and leptin is potently anti-steatotic (26–28). We next tested our hypothesis experimentally by immunoblot analysis of the liver tissues from our subcutaneous delivery experiment. This analysis revealed increased phosphorylation of AMPK α (Fig. 4A) and its downstream effector acetyl-CoA carboxylase (ACC, a central mediator of de novo fatty acid synthesis; Fig 4B) in 4-HPAA treated mice when compared to the scaffold control group. This observation was specific to the α subunit of AMPK, as subcutaneous 4-HPAA administration did not lead to the phosphorylation of the AMPK α subunit (Fig. S4).

173 To determine whether 4-HPAA can activate AMPK α in a cell autonomous manner we treated
174 primary mouse hepatocytes with physiologically relevant concentrations of 4-HPAA (0.01-10
175 μ M) for 30 minutes. Mirroring our *in vivo* observations, 4-HPAA treatment of primary mouse
176 hepatocytes lead to the phosphorylation of AMPK α and ACC in a dose-dependent manner *in*
177 *vitro* (Fig. 4C). Surprisingly, the peak phosphorylation of AMPK α was observed after treatment
178 with 1 μ M 4-HPAA, the same concentration as observed in the portal blood of our elderberry
179 extract-supplemented mice (Fig. 4C, 2E). These results indicate that 4-HPAA acts locally in the
180 liver –the primary site of accumulation– to activate AMPK α and downstream signaling events
181 that in turn activates fatty acid oxidation and blunts *de novo* lipogenesis.

182

183 **Flavonol catabolism is a rare feature among human microbiota**

184 While our berry-fed mice harbored flavonoid-catabolizing gut microbiota members capable of
185 producing 4-HPAA, clinical studies have shown that flavonoid catabolism is less prominent
186 among human gut microbiota and displays marked inter-individual variation (29, 30). Several
187 human gut commensals capable of catabolizing dietary flavonols into monophenolic acids have
188 been identified, the most studied example being the eponymous *Flavonifractor plautii* (formerly
189 *Clostridium oribscindens*) (Fig. S5) (15, 31). Notably, *F. plautii* belongs to the *Lachnospiraceae*
190 family, which accounted for one of the major changes in the microbiota of our berry
191 supplemented mice (Fig. 2C). Recently, the complete set of genes required for flavonol catabolic
192 activity was characterized. In total, four genes are required for the stepwise degradation of
193 flavones and flavonols into monophenolic acids such as 4-HPAA. These four genes encode a
194 flavone reductase (FLR), chalcone isomerase (CHI), enoate reductase (EnoR), and phloretin
195 hydrolase (PHY) (11–14) (Fig. 5A). To predict the flavonol catabolic capacity of human
196 metagenomes, we calculated the incidence of co-occurrence for this complete catabolic gene set
197 in the metagenomic sequencing data (n=1899 assemblies) from two publicly available
198 repositories (32, 33). Strikingly, although *F. plautii* was present in 28 percent of human
199 microbiomes in these datasets (Supplementary Tables 1,2), the incidence of any one catabolic
200 gene (>90% sequence similarity to the reference gene set) does not exceed 3 percent. Moreover,
201 the co-occurrence of all four genes –required for the complete flavonol degradation pathway– is
202 exceptionally rare, with an incidence of roughly one in two hundred (Fig. 5B). These data
203 suggest that not all *F. plautii* strains can catabolize flavonols and support the recent report that *F.*
204 *plautii* isolates are subject to inter-strain competition in the presence of flavonoids (34). Overall,
205 this highlights the rarity of a complete flavonol catabolic gene set in human microbiomes,
206 although the possibility exists that other catabolic pathways remain undiscovered.

207

208 Having deduced the predicted rarity of flavonol catabolizing genes in human metagenomes, we
209 next set out to test *in vitro* conversion of the flavonol kaempferol into 4-HPAA by stable human-
210 derived polymicrobial communities. In addition, we tested whether community converter
211 capacity could be induced by supplementation with an isolate of *F. plautii* with known flavonol
212 catabolizing capacity (Fig. 5C). In this experiment, we used a human-derived fecal microbiome
213 that lacked catabolic activity toward kaempferol as a negative control and scaffold community

214 into which we spiked in *F. plautii*. Following a 24-hour growth period in anaerobic conditions at
215 37° C, we provided either a vehicle control or kaempferol substrate and incubated the
216 communities for an additional 24 hours. Using a targeted LC-MS/MS approach to measure 4-
217 HPAA, the complete conversion of kaempferol substrate to 4-HPAA was observed in the *F.*
218 *plautii* containing community but not the scaffold negative control community. Together, these
219 data support our hypothesis that a single microbe with catabolic activity towards flavonoids can
220 be introduced into complex human fecal microbial communities to produce 4-HPAA *in vitro*,
221 creating perspective for use of *F. plautii* in probiotic interventions.

222

223 **Discussion**

224 Dietary intervention is a common approach to combat cardiometabolic disease (CMD), often
225 complementing traditional pharmaceutical therapies. The human gut microbiota extensively
226 metabolizes dietary input, yielding a plethora of microbe-derived metabolites with poorly
227 characterized influences on host physiology. Pertinent to this study, dietary flavonoids have been
228 reported to abrogate diet-induced obesity in a microbe-dependent manner (8, 9). Moreover,
229 several commensal gut bacteria are known to catabolize flavonoids into monophenolic acids
230 (15). However, the contribution of these diet-derived gut microbial metabolites to CMD remains
231 unclear. In an effort to understand the role of microbial flavonoid catabolites in obesity-related
232 CMD, we used a multifaceted approach to study the interface of diet, the gut microbiota, and
233 host physiology with single-molecule resolution.

234

235 Our study uncovers the functional importance of a single flavonoid-derived microbial catabolite,
236 4-HPAA, in abrogating HFD-induced hepatic steatosis. In addition, we establish the ability of 4-
237 HPAA to activate AMPK α and modulate its downstream effectors. Remarkably, our
238 investigation of the presence of *F. plautii* flavone/flavonol catabolizing (4-HPAA producing)
239 genes present in human metagenomic data revealed that although 28 percent of the 1,899
240 assemblies contained any one particular strain of *F. plautii*, less than one half of one percent
241 contained all four genes required to produce 4-HPAA from a flavonoid precursor. Paired with
242 the notable intra-individual variation of flavonoid catabolic activity in humans (29, 30), these
243 data underscore the need to consider the microbial contribution to dietary intervention as a
244 complementary strategy to combat CMD. Stratification by “responder” status based on the co-
245 occurrence of the complete flavonoid catabolizing gene set may inform, in part, the efficacy of
246 intervention. While theoretically possible, the ability of a probiotic flavonoid-catabolizing *F.*
247 *plautii* strain to stably colonize the gut remains to be determined and may prove challenging due
248 to strain level competition, particularly in the presence of a flavonoid substrate (34), and the
249 frequency of non-synonymous mutations over time (35). As an alternative, additional flavonoid-
250 catabolizing microbiota members can be isolated and characterized or a next generation synbiotic
251 could be engineered by inserting the flavonoid-catabolizing gene set into a stably colonizing
252 commensal host.

253

254 Our study has several limitations. First, studying human-relevant dietary substrates in a mouse
255 model is reductive in that the human and mouse microbiota are not entirely comparable entities
256 (36). Consequently, the development of humanized gnotobiotic mouse models have served as a
257 welcomed advance in the study of diet-gut microbiota interactions (37). However, even this
258 state-of-the-art approach has its own limitations as the colonization of the complete donor
259 community is often not possible due to specific microbe-host dependencies (37). Second, since
260 germ-free mice are resistant to diet-induced obesity (38), we were unable to test the anti-
261 obesogenic properties of elderberry extract-supplemented HFD or 4-HPAA in the absence of the
262 gut microbiota. Third, the possibility exists that undiscovered bacterial catabolic pathways may
263 catabolize flavones/flavonols into 4-HPAA. To this point, we simply used the knowledge at our
264 disposal, focusing on the known catabolic pathway. Lastly, although the subcutaneous
265 administration provides a high level of resolution, this approach discounts the physiological
266 circulation of gut microbial metabolites, first draining through the mesentery into the portal vein
267 before delivery to the liver. Future studies can overcome this challenge by continuously infusing
268 metabolites of interest directly into the portal vein, mirroring the natural circulation of microbial
269 metabolites *in vivo* (18).

270
271 In conclusion, we used an array of *in vitro*, *in vivo*, and *in silico* analyses to reveal the gut
272 microbial contribution of flavonoid catabolism in the context of overnutrition-induced metabolic
273 disease and identified 4-HPAA, a single microbe-derived metabolite sufficient to abrogate
274 obesity-driven hepatic steatosis. We see this as an example of how a single gut microbial
275 metabolite stemming from the diet can profoundly impact host physiology and is a step towards
276 combined diet-probiotic intervention therapies for cardiometabolic diseases.

277

278 **References and Notes**

- 279 1. Z. Wang, E. Klipfell, B. J. Bennett, R. Koeth, B. S. Levison, B. Dugar, A. E. Feldstein, E.
280 B. Britt, X. Fu, Y.-M. Chung, Y. Wu, P. Schauer, J. D. Smith, H. Allayee, W. H. W.
281 Tang, J. A. DiDonato, A. J. Lusis, S. L. Hazen, Gut flora metabolism of
282 phosphatidylcholine promotes cardiovascular disease. *Nature*. 472, 57–63 (2011).
- 283 2. A. Koh, A. Molinaro, M. Ståhlman, M. T. Khan, C. Schmidt, L. Mannerås-Holm, H. Wu,
284 A. Carreras, H. Jeong, L. E. Olofsson, P.-O. Bergh, V. Gerdes, A. Hartstra, M. de Brauw,
285 R. Perkins, M. Nieuwdorp, G. Bergström, F. Bäckhed, Microbially Produced Imidazole
286 Propionate Impairs Insulin Signaling through mTORC1. *Cell*. 175, 947-961.e17 (2018).
- 287 3. N. P. Bondonno, F. Dalgaard, C. Kyrø, K. Murray, C. P. Bondonno, J. R. Lewis, K. D.
288 Croft, G. Gislason, A. Scalbert, A. Cassidy, A. Tjønneland, K. Overvad, J. M. Hodgson,
289 Flavonoid intake is associated with lower mortality in the Danish Diet Cancer and Health
290 Cohort. *Nature Communications*. 10, 3651 (2019).
- 291 4. Wang Dong D., Li Yanping, Bhupathiraju Shilpa N., Rosner Bernard A., Sun Qi,
292 Giovannucci Edward L., Rimm Eric B., Manson JoAnn E., Willett Walter C., Stampfer
293 Meir J., Hu Frank B., Fruit and Vegetable Intake and Mortality: Results From 2

- 294 Prospective Cohort Studies of US Men and Women and a Meta-Analysis of 26 Cohort
295 Studies. *Circulation*. 0, doi:10.1161/CIRCULATIONAHA.120.048996.
- 296 5. A. S. Go, D. Mozaffarian, V. L. Roger, E. J. Benjamin, J. D. Berry, W. B. Borden, D. M.
297 Bravata, S. Dai, E. S. Ford, C. S. Fox, S. Franco, H. J. Fullerton, C. Gillespie, S. M.
298 Hailpern, J. A. Heit, V. J. Howard, M. D. Huffman, B. M. Kissela, S. J. Kittner, D. T.
299 Lackland, J. H. Lichtman, L. D. Lisabeth, D. Magid, G. M. Marcus, A. Marelli, D. B.
300 Matchar, D. K. McGuire, E. R. Mohler, C. S. Moy, M. E. Mussolino, G. Nichol, N. P.
301 Paynter, P. J. Schreiner, P. D. Sorlie, J. Stein, T. N. Turan, S. S. Virani, N. D. Wong, D.
302 Woo, M. B. Turner, American Heart Association Statistics Committee and Stroke
303 Statistics Subcommittee, Heart disease and stroke statistics--2013 update: a report from
304 the American Heart Association. *Circulation*. 127, e6–e245 (2013).
- 305 6. G. Williamson, C. D. Kay, A. Crozier, The Bioavailability, Transport, and Bioactivity of
306 Dietary Flavonoids: A Review from a Historical Perspective. *Comprehensive Reviews in*
307 *Food Science and Food Safety*. 17, 1054–1112 (2018).
- 308 7. L. J. Osborn, J. Claesen, J. M. Brown, Microbial Flavonoid Metabolism: A
309 Cardiometabolic Disease Perspective. *Annual Review of Nutrition*. 41 (2021),
310 doi:10.1146/annurev-nutr-120420-030424.
- 311 8. L. A. David, C. F. Maurice, R. N. Carmody, D. B. Gootenberg, J. E. Button, B. E. Wolfe,
312 A. V. Ling, A. S. Devlin, Y. Varma, M. A. Fischbach, S. B. Biddinger, R. J. Dutton, P. J.
313 Turnbaugh, Diet rapidly and reproducibly alters the human gut microbiome. *Nature*. 505,
314 559–563 (2014).
- 315 9. R. A. Koeth, Z. Wang, B. S. Levison, J. A. Buffa, E. Org, B. T. Sheehy, E. B. Britt, X.
316 Fu, Y. Wu, L. Li, J. D. Smith, J. A. DiDonato, J. Chen, H. Li, G. D. Wu, J. D. Lewis, M.
317 Warriar, J. M. Brown, R. M. Krauss, W. H. W. Tang, F. D. Bushman, A. J. Lusis, S. L.
318 Hazen, Intestinal microbiota metabolism of l-carnitine, a nutrient in red meat, promotes
319 atherosclerosis. *Nat Med*. 19, 576–585 (2013).
- 320 10. W. H. W. Tang, Z. Wang, B. S. Levison, R. A. Koeth, E. B. Britt, X. Fu, Y. Wu, S. L.
321 Hazen, Intestinal Microbial Metabolism of Phosphatidylcholine and Cardiovascular Risk.
322 *N Engl J Med*. 368, 1575–1584 (2013).
- 323 11. J. Tan, C. McKenzie, M. Potamitis, A. N. Thorburn, C. R. Mackay, L. Macia, The role of
324 short-chain fatty acids in health and disease. *Adv Immunol*. 121, 91–119 (2014).
- 325 12. A. C. Burke, B. G. Sutherland, D. E. Telford, M. R. Morrow, C. G. Sawyez, J. Y.
326 Edwards, M. Drangova, M. W. Huff, *J. Lipid Res.*, in press, doi:10.1194/jlr.M087387.
- 327 13. D. Esposito, T. Damsud, M. Wilson, M. H. Grace, R. Strauch, X. Li, M. A. Lila (18), S.
328 Komarnytsky, Black Currant Anthocyanins Attenuate Weight Gain and Improve Glucose
329 Metabolism in Diet-Induced Obese Mice with Intact, but Not Disrupted, Gut
330 Microbiome. *Journal of Agricultural and Food Chemistry*. 63, 6172–6180 (2015).
- 331 14. J. Winter, L. H. Moore, V. R. Dowell, V. D. Bokkenheuser, C-Ring Cleavage of
332 Flavonoids by Human Intestinal Bacteria. *APPL. ENVIRON. MICROBIOL*. 55, 6
333 (1989).
- 334 15. C. Herles, A. Braune, M. Blaut, First bacterial chalcone isomerase isolated from
335 *Eubacterium ramulus*. *Arch Microbiol*. 181, 428–434 (2004).

- 336 16. A. Braune, M. Gütschow, M. Blaut, An NADH-Dependent Reductase from *Eubacterium*
337 *ramulus* Catalyzes the Stereospecific Heteroring Cleavage of Flavanones and
338 Flavanonols. *Appl. Environ. Microbiol.* 85 (2019), doi:10.1128/AEM.01233-19.
- 339 17. L. Schoefer, A. Braune, M. Blaut, Cloning and Expression of a Phloretin Hydrolase Gene
340 from *Eubacterium ramulus* and Characterization of the Recombinant Enzyme. *Appl*
341 *Environ Microbiol.* 70, 6131–6137 (2004).
- 342 18. G. Yang, S. Hong, P. Yang, Y. Sun, Y. Wang, P. Zhang, W. Jiang, Y. Gu, Discovery of
343 an ene-reductase for initiating flavone and flavonol catabolism in gut bacteria. *Nature*
344 *Communications.* 12, 790 (2021).
- 345 19. L. Hoyles, J.-M. Fernández-Real, M. Federici, M. Serino, J. Abbott, J. Charpentier, C.
346 Heymes, J. L. Luque, E. Anthony, R. H. Barton, J. Chilloux, A. Myridakis, L. Martinez-
347 Gili, J. M. Moreno-Navarrete, F. Benhamed, V. Azalbert, V. Blasco-Baque, J. Puig, G.
348 Xifra, W. Ricart, C. Tomlinson, M. Woodbridge, M. Cardellini, F. Davato, I. Cardolini,
349 O. Porzio, P. Gentileschi, F. Lopez, F. Fougelle, S. A. Butcher, E. Holmes, J. K.
350 Nicholson, C. Postic, R. Burcelin, M.-E. Dumas, Molecular Phenomics and
351 Metagenomics of Hepatic Steatosis in Non-Diabetic Obese Women. *Nat Med.* 24, 1070–
352 1080 (2018).
- 353 20. J. Ukropec, R. P. Anunciado, Y. Ravussin, M. W. Hulver, L. P. Kozak, UCP1-
354 independent Thermogenesis in White Adipose Tissue of Cold-acclimated *Ucp1*^{-/-} Mice
355 *. *Journal of Biological Chemistry.* 281, 31894–31908 (2006).
- 356 21. D. Orabi, L. J. Osborn, K. Fung, W. Massey, A. J. Horak III, F. Aucejo, I. Choucair, B.
357 DeLucia, Z. Wang, J. Claesen, J. M. Brown, A surgical method for continuous intraportal
358 infusion of gut microbial metabolites in mice. *JCI Insight.* 6, e145607 (2021).
- 359 22. K. W. Cho, Y. Zhou, L. Sheng, L. Rui, Lipocalin-13 Regulates Glucose Metabolism by
360 both Insulin-Dependent and Insulin-Independent Mechanisms. *Molecular and Cellular*
361 *Biology.* 31, 450–457 (2011).
- 362 23. L. Sheng, K. W. Cho, Y. Zhou, H. Shen, L. Rui, Lipocalin 13 protein protects against
363 hepatic steatosis by both inhibiting lipogenesis and stimulating fatty acid β -oxidation. *J.*
364 *Biol. Chem.* 286, 38128–38135 (2011).
- 365 24. Y. Zhou, L. Rui, LIPOCALIN 13 REGULATION OF GLUCOSE AND LIPID
366 METABOLISM IN OBESITY. *Vitam Horm.* 91, 369–383 (2013).
- 367 25. K. V. Doan, C. M. Ko, A. W. Kinyua, D. J. Yang, Y.-H. Choi, I. Y. Oh, N. M. Nguyen,
368 A. Ko, J. W. Choi, Y. Jeong, M. H. Jung, W. G. Cho, S. Xu, K. S. Park, W. J. Park, S. Y.
369 Choi, H. S. Kim, S. H. Moh, K. W. Kim, Gallic acid regulates body weight and glucose
370 homeostasis through AMPK activation. *Endocrinology.* 156, 157–168 (2015).
- 371 26. Y. Jung, J. Park, H.-L. Kim, J.-E. Sim, D.-H. Youn, J. Kang, S. Lim, M.-Y. Jeong, W. M.
372 Yang, S.-G. Lee, K. S. Ahn, J.-Y. Um, Vanillic acid attenuates obesity via activation of
373 the AMPK pathway and thermogenic factors in vivo and in vitro. *The FASEB Journal.*
374 32, 1388–1402 (2018).
- 375 27. C.-C. Liao, T.-T. Ou, C.-H. Wu, C.-J. Wang, Prevention of diet-induced hyperlipidemia
376 and obesity by caffeic acid in C57BL/6 mice through regulation of hepatic lipogenesis
377 gene expression. *J Agric Food Chem.* 61, 11082–11088 (2013).

- 378 28. M. M. Mihaylova, R. J. Shaw, The AMPK signalling pathway coordinates cell growth,
379 autophagy and metabolism. *Nat Cell Biol.* 13, 1016–1023 (2011).
- 380 29. Y. C. Long, J. R. Zierath, AMP-activated protein kinase signaling in metabolic
381 regulation. *J Clin Invest.* 116, 1776–1783 (2006).
- 382 30. P. Zhao, A. R. Saltiel, From overnutrition to liver injury: AMP-activated protein kinase in
383 nonalcoholic fatty liver diseases. *J Biol Chem.* 295, 12279–12289 (2020).
- 384 31. B. K. Smith, K. Marcinko, E. M. Desjardins, J. S. Lally, R. J. Ford, G. R. Steinberg,
385 Treatment of nonalcoholic fatty liver disease: role of AMPK. *Am J Physiol Endocrinol*
386 *Metab.* 311, E730–E740 (2016).
- 387 32. A. R. Rechner, M. A. Smith, G. Kuhnle, G. R. Gibson, E. S. Debnam, S. K. S. Srail, K. P.
388 Moore, C. A. Rice-Evans, Colonic metabolism of dietary polyphenols: influence of
389 structure on microbial fermentation products. *Free Radical Biology and Medicine.* 36,
390 212–225 (2004).
- 391 33. A. Cassidy, A.-M. Minihane, The role of metabolism (and the microbiome) in defining
392 the clinical efficacy of dietary flavonoids. *Am J Clin Nutr.* 105, 10–22 (2017).
- 393 34. J. Winter, M. R. Popoff, P. Grimont, V. D. Bokkenheuser, *Clostridium orbiscindens* sp.
394 nov., a human intestinal bacterium capable of cleaving the flavonoid C-ring. *Int. J. Syst.*
395 *Bacteriol.* 41, 355–357 (1991).
- 396 35. M. Poyet, M. Groussin, S. M. Gibbons, J. Avila-Pacheco, X. Jiang, S. M. Kearney, A. R.
397 Perrotta, B. Berdy, S. Zhao, T. D. Lieberman, P. K. Swanson, M. Smith, S. Roesemann,
398 J. E. Alexander, S. A. Rich, J. Livny, H. Vlamakis, C. Clish, K. Bullock, A. Deik, J.
399 Scott, K. A. Pierce, R. J. Xavier, E. J. Alm, A library of human gut bacterial isolates
400 paired with longitudinal multiomics data enables mechanistic microbiome research.
401 *Nature Medicine.* 25, 1442–1452 (2019).
- 402 36. Y. Zou, W. Xue, G. Luo, Z. Deng, P. Qin, R. Guo, H. Sun, Y. Xia, S. Liang, Y. Dai, D.
403 Wan, R. Jiang, L. Su, Q. Feng, Z. Jie, T. Guo, Z. Xia, C. Liu, J. Yu, Y. Lin, S. Tang, G.
404 Huo, X. Xu, Y. Hou, X. Liu, J. Wang, H. Yang, K. Kristiansen, J. Li, H. Jia, L. Xiao,
405 1,520 reference genomes from cultivated human gut bacteria enable functional
406 microbiome analyses. *Nature Biotechnology.* 37, 179–185 (2019).
- 407 37. G. P. Rodriguez-Castaño, F. E. Rey, A. Caro-Quintero, A. Acosta-González, Gut-derived
408 Flavonifractor species variants are differentially enriched during in vitro incubation with
409 quercetin. *PLOS ONE.* 15, e0227724 (2020).
- 410 38. B. Yilmaz, C. Mooser, I. Keller, H. Li, J. Zimmermann, L. Bosshard, T. Fuhrer, M.
411 Gomez de Agüero, N. F. Trigo, H. Tschanz-Lischer, J. P. Limenitakis, W.-D. Hardt, K.
412 D. McCoy, B. Stecher, L. Excoffier, U. Sauer, S. C. Ganal-Vonarburg, A. J. Macpherson,
413 Long-term evolution and short-term adaptation of microbiota strains and sub-strains in
414 mice. *Cell Host & Microbe.* 29, 650-663.e9 (2021).
- 415 39. T. L. A. Nguyen, S. Vieira-Silva, A. Liston, J. Raes, How informative is the mouse for
416 human gut microbiota research? *Dis Model Mech.* 8, 1–16 (2015).
- 417 40. J. C. Park, S.-H. Im, Of men in mice: the development and application of a humanized
418 gnotobiotic mouse model for microbiome therapeutics. *Experimental & Molecular*
419 *Medicine.* 52, 1383–1396 (2020).

- 420 41. F. Bäckhed, J. K. Manchester, C. F. Semenkovich, J. I. Gordon, Mechanisms underlying
421 the resistance to diet-induced obesity in germ-free mice. *Proc. Natl. Acad. Sci. U.S.A.*
422 104, 979–984 (2007).
- 423 42. R. N. Helsley, V. Venkateshwari, A. L. Brown, A. D. Gromovsky, R. C. Schugar, I.
424 Ramachandiran, K. Fung, M. N. Kabbany, R. Banerjee, C. K. Neumann, C. Finney, P.
425 Pathak, O. Danny, L. J. Osborn, W. Massey, R. Zhang, A. Kadam, B. E. Sansbury, C.
426 Pan, J. Sacks, R. G. Lee, R. M. Croke, M. J. Graham, M. E. Lemieux, V. Gogonea, J. P.
427 Kirwan, D. S. Allende, M. Civelek, P. L. Fox, L. L. Rudel, A. J. Lusic, M. Spite, J. M.
428 Brown, Obesity-linked suppression of membrane-bound O-Acyltransferase 7 (MBOAT7)
429 drives non-alcoholic fatty liver disease. *eLife*. 8, e49882 (2019).
- 430 43. C. J. Gordon, The mouse thermoregulatory system: Its impact on translating biomedical
431 data to humans. *Physiol Behav.* 179, 55–66 (2017).
- 432 44. A. I. Mina, R. A. LeClair, K. B. LeClair, D. E. Cohen, L. Lantier, A. S. Banks, CalR: A
433 Web-Based Analysis Tool for Indirect Calorimetry Experiments. *Cell Metab.* 28, 656-
434 666.e1 (2018).
- 435 45. J. G. Caporaso, J. Kuczynski, J. Stombaugh, K. Bittinger, F. D. Bushman, E. K. Costello,
436 N. Fierer, A. G. Peña, J. K. Goodrich, J. I. Gordon, G. A. Huttley, S. T. Kelley, D.
437 Knights, J. E. Koenig, R. E. Ley, C. A. Lozupone, D. McDonald, B. D. Muegge, M.
438 Pirrung, J. Reeder, J. R. Sevinsky, P. J. Turnbaugh, W. A. Walters, J. Widmann, T.
439 Yatsunenko, J. Zaneveld, R. Knight, QIIME allows analysis of high-throughput
440 community sequencing data. *Nat Methods.* 7, 335–336 (2010).
- 441 46. B. J. Callahan, P. J. McMurdie, M. J. Rosen, A. W. Han, A. J. A. Johnson, S. P. Holmes,
442 DADA2: High-resolution sample inference from Illumina amplicon data. *Nat Methods.*
443 13, 581–583 (2016).
- 444 47. P. J. McMurdie, S. Holmes, phyloseq: an R package for reproducible interactive analysis
445 and graphics of microbiome census data. *PLoS One.* 8, e61217 (2013).
- 446 48. P. J. McMurdie, S. Holmes, Waste not, want not: why rarefying microbiome data is
447 inadmissible. *PLoS Comput Biol.* 10, e1003531 (2014).
- 448 49. H. Wickham, *ggplot2: Elegant Graphics for Data Analysis* (Springer Publishing
449 Company, Incorporated, 2009; <https://ggplot2-book.org/>).
- 450 50. Y. Benjamini, Y. Hochberg, Controlling the False Discovery Rate: A Practical and
451 Powerful Approach to Multiple Testing. *Journal of the Royal Statistical Society. Series B*
452 (Methodological). 57, 289–300 (1995).
- 453 51. E.-M. Tiit, *Nonparametric Statistical Methods*. Myles Hollander and Douglas A. Wolfe,
454 Wiley, Chichester, 1999. No. of pages: xiii+779. Price: £ 39.95. ISBN 0-471-19045-4.
455 *Statistics in Medicine.* 19, 1386–1388 (2000).
- 456 52. J. P. Buchmann, E. C. Holmes, Entrezpy: a Python library to dynamically interact with
457 the NCBI Entrez databases. *Bioinformatics.* 35, 4511–4514 (2019).
- 458 53. D. T. Truong, E. A. Franzosa, T. L. Tickle, M. Scholz, G. Weingart, E. Pasolli, A. Tett,
459 C. Huttenhower, N. Segata, MetaPhlan2 for enhanced metagenomic taxonomic profiling.
460 *Nat Methods.* 12, 902–903 (2015).

- 461 54. D. Li, C.-M. Liu, R. Luo, K. Sadakane, T.-W. Lam, MEGAHIT: an ultra-fast single-node
462 solution for large and complex metagenomics assembly via succinct de Bruijn graph.
463 *Bioinformatics*. 31, 1674–1676 (2015).
- 464 55. Y. Liao, G. K. Smyth, W. Shi, featureCounts: an efficient general purpose program for
465 assigning sequence reads to genomic features. *Bioinformatics*. 30, 923–930 (2014).
- 466 56. Y. Liao, G. K. Smyth, W. Shi, The R package Rsubread is easier, faster, cheaper and
467 better for alignment and quantification of RNA sequencing reads. *Nucleic Acids Res.* 47,
468 e47 (2019).
- 469 57. R. L. McCullough, M. R. McMullen, D. Das, S. Roychowdhury, M. G. Strainic, M. E.
470 Medof, L. E. Nagy, Differential contribution of complement receptor C5aR in myeloid
471 and non-myeloid cells in chronic ethanol-induced liver injury in mice. *Mol Immunol.* 75,
472 122–132 (2016).
- 473 58. J. M. Brown, M. S. Boysen, S. Chung, O. Fabiyi, R. F. Morrison, S. Mandrup, M. K.
474 McIntosh, Conjugated linoleic acid induces human adipocyte delipidation:
475 autocrine/paracrine regulation of MEK/ERK signaling by adipocytokines. *J Biol Chem.*
476 279, 26735–26747 (2004).
- 477 59. K. A. Romano, K. A. Dill-McFarland, K. Kasahara, R. L. Kerby, E. I. Vivas, D. Amador-
478 Noguez, P. Herd, F. E. Rey, Fecal Aliquot Straw Technique (FAST) allows for easy and
479 reproducible subsampling: assessing interpersonal variation in trimethylamine-N-oxide
480 (TMAO) accumulation. *Microbiome*. 6 (2018), doi:10.1186/s40168-018-0458-8.
- 481 60. T. D. Wilkins, S. Chalgren, Medium for use in antibiotic susceptibility testing of
482 anaerobic bacteria. *Antimicrob Agents Chemother.* 10, 926–928 (1976).
- 483 61. A. Gotoh, M. Nara, Y. Sugiyama, M. Sakanaka, H. Yachi, A. Kitakata, A. Nakagawa, H.
484 Minami, S. Okuda, T. Katoh, T. Katayama, S. Kurihara, Use of Gifu Anaerobic Medium
485 for culturing 32 dominant species of human gut microbes and its evaluation based on
486 short-chain fatty acids fermentation profiles. *Bioscience, Biotechnology, and*
487 *Biochemistry*. 81, 2009–2017 (2017).
- 488 62. A. M. Bolger, M. Lohse, B. Usadel, Trimmomatic: a flexible trimmer for Illumina
489 sequence data. *Bioinformatics*. 30, 2114–2120 (2014).
- 490 63. A. Prjibelski, D. Antipov, D. Meleshko, A. Lapidus, A. Korobeynikov, Using SPAdes De
491 Novo Assembler. *Current Protocols in Bioinformatics*. 70, e102 (2020).
- 492 64. T. Seemann, Prokka: rapid prokaryotic genome annotation. *Bioinformatics*. 30, 2068–
493 2069 (2014).
- 494 65. J. J. Davis, A. R. Wattam, R. K. Aziz, T. Brettin, R. Butler, R. M. Butler, P. Chlenski, N.
495 Conrad, A. Dickerman, E. M. Dietrich, J. L. Gabbard, S. Gerdes, A. Guard, R. W.
496 Kenyon, D. Machi, C. Mao, D. Murphy-Olson, M. Nguyen, E. K. Nordberg, G. J. Olsen,
497 R. D. Olson, J. C. Overbeek, R. Overbeek, B. Parrello, G. D. Pusch, M. Shukla, C.
498 Thomas, M. VanOeffelen, V. Vonstein, A. S. Warren, F. Xia, D. Xie, H. Yoo, R.
499 Stevens, The PATRIC Bioinformatics Resource Center: expanding data and analysis
500 capabilities. *Nucleic Acids Res.* 48, D606–D612 (2020).
- 501 66. T. Brettin, J. J. Davis, T. Disz, R. A. Edwards, S. Gerdes, G. J. Olsen, R. Olson, R.
502 Overbeek, B. Parrello, G. D. Pusch, M. Shukla, J. A. Thomason, R. Stevens, V. Vonstein,

- 503 A. R. Wattam, F. Xia, RASTtk: A modular and extensible implementation of the RAST
504 algorithm for building custom annotation pipelines and annotating batches of genomes.
505 *Sci Rep.* 5 (2015), doi:10.1038/srep08365.
- 506 67. B. D. Ondov, T. J. Treangen, P. Melsted, A. B. Mallonee, N. H. Bergman, S. Koren, A.
507 M. Phillippy, Mash: fast genome and metagenome distance estimation using MinHash.
508 *Genome Biology.* 17, 132 (2016).
- 509 68. J. J. Davis, S. Gerdes, G. J. Olsen, R. Olson, G. D. Pusch, M. Shukla, V. Vonstein, A. R.
510 Wattam, H. Yoo, PATtyFams: Protein Families for the Microbial Genomes in the
511 PATRIC Database. *Front Microbiol.* 7, 118 (2016).
- 512 69. R. C. Edgar, MUSCLE: multiple sequence alignment with high accuracy and high
513 throughput. *Nucleic Acids Res.* 32, 1792–1797 (2004).
- 514 70. A. Stamatakis, RAxML version 8: a tool for phylogenetic analysis and post-analysis of
515 large phylogenies. *Bioinformatics.* 30, 1312–1313 (2014).
- 516 71. A. Stamatakis, P. Hoover, J. Rougemont, A rapid bootstrap algorithm for the RAxML
517 Web servers. *Syst Biol.* 57, 758–771 (2008).

518

519 **Acknowledgments:** We would like to thank Brandon Stelter from the Cleveland Clinic Center
520 for Medical Art and Photography for creating the graphical abstract.

521

522 **Funding:**

523 National Institutes of Health grant T32 GM088088 (LJO)
524 National Institutes of Health grant R01 AI153173 (JC)
525 National Institutes of Health grant R01 HL120679 (JMB)
526 National Institutes of Health grant R01 DK130227 (JMB)
527 National Institutes of Health grant P01 HL147823 (AMH, ZW, JMB, SLH)
528 National Institutes of Health grant P50 AA024333 (LEN, DSA, JMB)
529 National Institutes of Health grant U01 AA026938 (LEN, JMB)
530 Research Grant from the Prevent Cancer Foundation PCF2019-JC (JC)
531 American Cancer Society Institutional Research Grant IRG-16-186-21 (JC)
532 Case Comprehensive Cancer Center Jump Start Award CA043703 (JC)

533

534 **Author contributions:**

535 Conceptualization: LJO, JMB, JC
536 Methodology: LJO, AMH, CM, PPA, JMB, JC
537 Investigation: LJO, KS, WM, BD, IC, VV, KF, AJH, DO, IN, DSA, NS
538 Visualization: LJO, JC
539 Funding acquisition: LJO, LEN, ZW, DSA, AMH, SLH, JMB, JC
540 Writing – original draft: LJO
541 Writing – review & editing: All authors

542

543 **Competing interests:** JC is a Scientific Advisor for Seed Health, Inc. ZW and SLH report being
544 named as co-inventor on pending and issued patents held by the Cleveland Clinic relating to

545 cardiovascular diagnostics and therapeutics. SLH reports being a paid consultant for Procter &
546 Gamble, and Zehna Therapeutics, having received research funds from Procter & Gamble,
547 Roche Diagnostics and Zehna therapeutics, and being eligible to receive royalty payments for
548 inventions or discoveries related to cardiovascular diagnostics or therapeutics from Cleveland
549 Heart Lab, a fully owned subsidiary of Quest Diagnostics, and Procter & Gamble. The other
550 authors declare they have no competing interests.
551

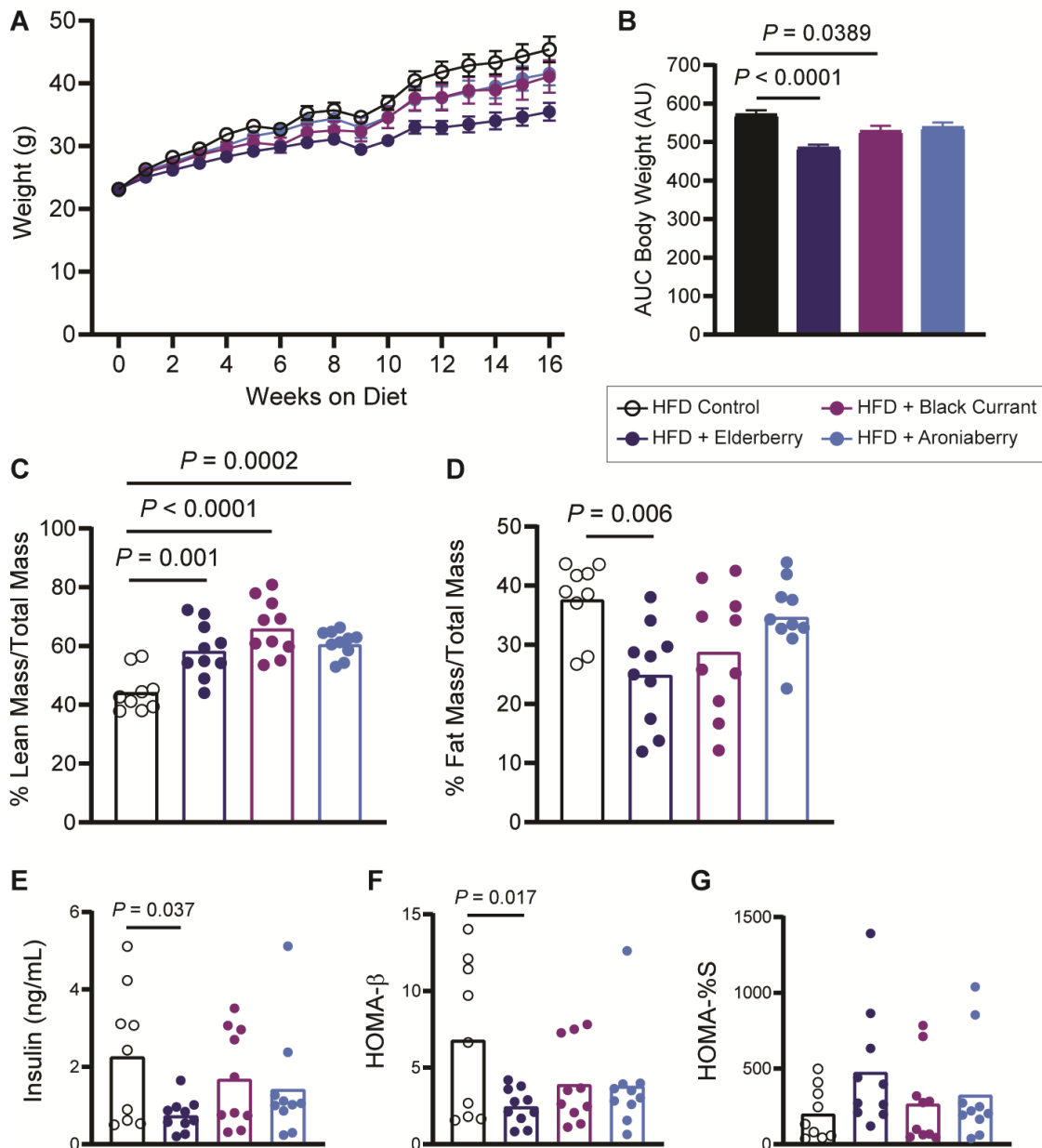
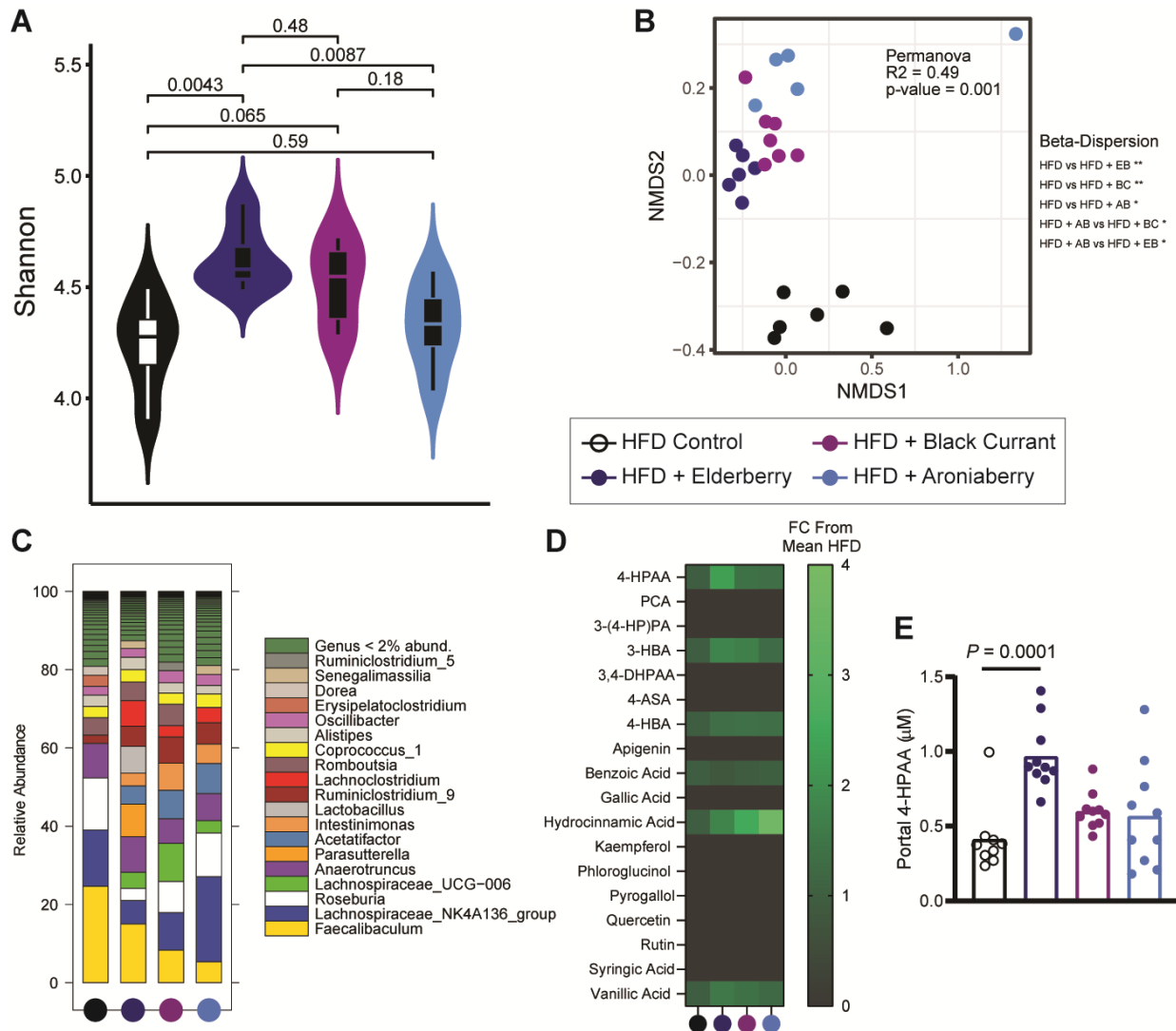


Fig. 1. Berry extract supplements reduce high fat diet-induced obesity. **(A)** Body weights of 6-week-old male C57BL/6 mice fed a high fat control diet, or the same diet supplemented with 1% w/w elderberry, black currant, or aroniaberry extracts for 16 weeks; n=9-10 per group, error bars represent SEM. **(B)** Mean cumulative area under the curve (AUC) for body weights after 16 weeks, error bars represent SEM. **(C) and (D)** Lean and fat mass after 16 weeks as measured by EchoMRI and normalized to total body mass, n=9-10 per group. **(E)** Plasma insulin after 16 weeks on either control or experimental diets following a 4-hour fast, n=9-10 per group. **(F)** Homeostatic model assessment of β -cell function (HOMA- β), n=9-10 per group. **(G)** Percent insulin sensitivity after 16 weeks, n=9-10 per group. Individual points represent individual mice, and bars represent group means. All *P* values shown were calculated using one-way ANOVA with Dunnett's multiple comparisons test; n=9-10 per group.

552
553
554
555
556
557
558
559
560
561
562
563
564
565

566



567

568

569

570

571

572

573

574

575

576

577

578

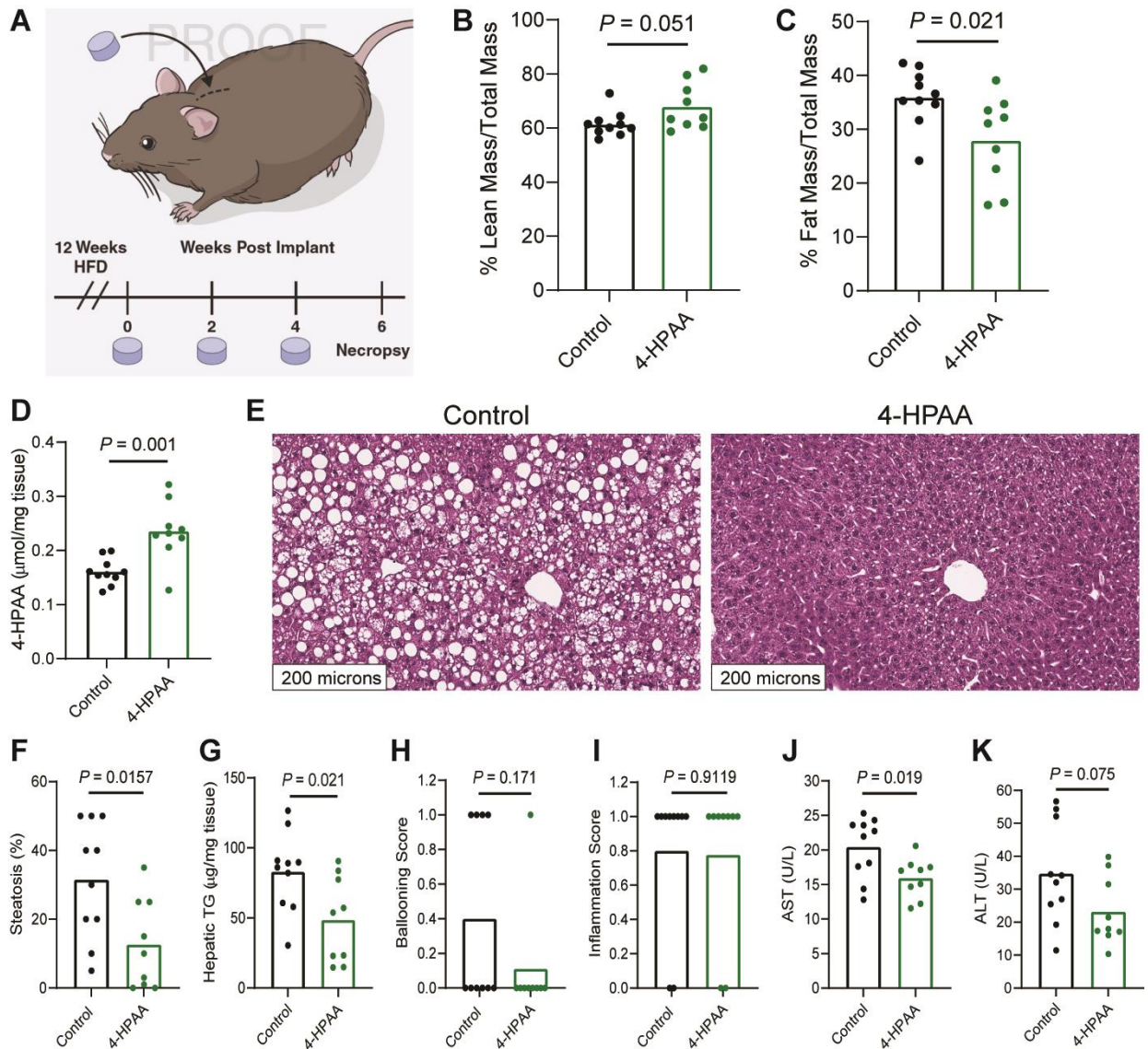
579

580

581

Fig. 2. Berry extracts alter the cecal microbiome. (A) Shannon alpha diversity estimates for cecal microbiomes based on 16S rRNA profiles of all four groups. Statistical analysis was performed via ANOVA. (B) NMDS plots based on the Bray-Curtis index between the cecal 16S rRNA profile of all four groups. Statistical analysis was performed with PERMANOVA where R2 values are noted for comparisons with significant p-values and stand for percentage variance explained by the variable of interest. (C) Stacked bar chart of relative abundance (left y-axis) of the top 20 genera assembled across the cecal 16S rRNA profiles of all four groups. n=6 for all 16S rRNA sequencing analysis. (D) Heatmap of portal plasma flavonoids and microbial flavonoid catabolites measured by LC-MS/MS, n=9-10 per group. (E) Portal plasma concentration of the microbial flavonol catabolite 4-HPAA measured by LC-MS/MS, one-way ANOVA with Dunnett's multiple comparisons test; n=9-10 per group. Individual points represent individual mice, and bars represent group means.

582



583

584

585

586

587

588

589

590

591

592

593

594

595

596

597

598

Fig. 3. 4-HPAA is sufficient to reverse HFD-induced hepatic steatosis and liver injury. (A) 4-week-old male C57BL/6 mice were fed a high fat diet for 12 weeks to induce obesity. After the induction of diet-induced obesity, mice were randomly assigned to receive a subcutaneously implanted control scaffold pellet, or a pellet releasing 350 μg 4-HPAA per day for two weeks. New pellets were implanted every two weeks for a total of 6 weeks. Lean mass (B) and fat mass (C) were measured by Echo MRI, $n=9-10$ per group. (D) 4-HPAA accumulates in the liver as measured by LC-MS/MS, $n=9-10$ per group. (E-G) After a total of 18 weeks of high fat diet feeding, H&E-stained sections of liver revealed profound hepatic steatosis in scaffold control mice while 4-HPAA treated mice had marked reversal of steatosis and triglyceride deposition $n=6-10$ per group. Histologic assessment of hepatocellular ballooning (H) and inflammation (I), $n=6$ per group. (J, K) Quantification of liver injury biomarkers in peripheral plasma, $n=9-10$ per group. Statistical analysis was performed using unpaired two-tailed Student's t-test. Individual points represent individual mice, and bars represent group means.

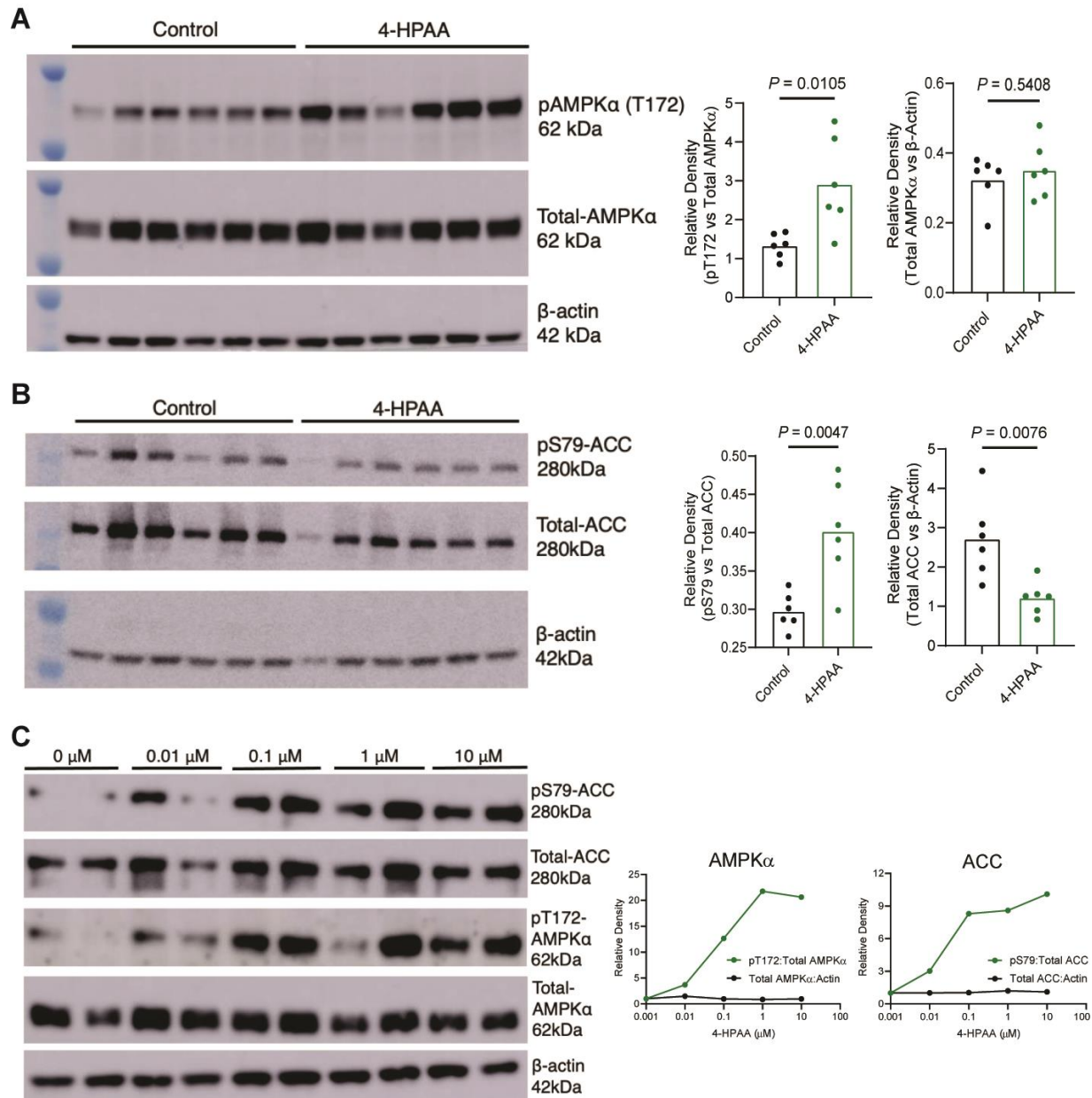
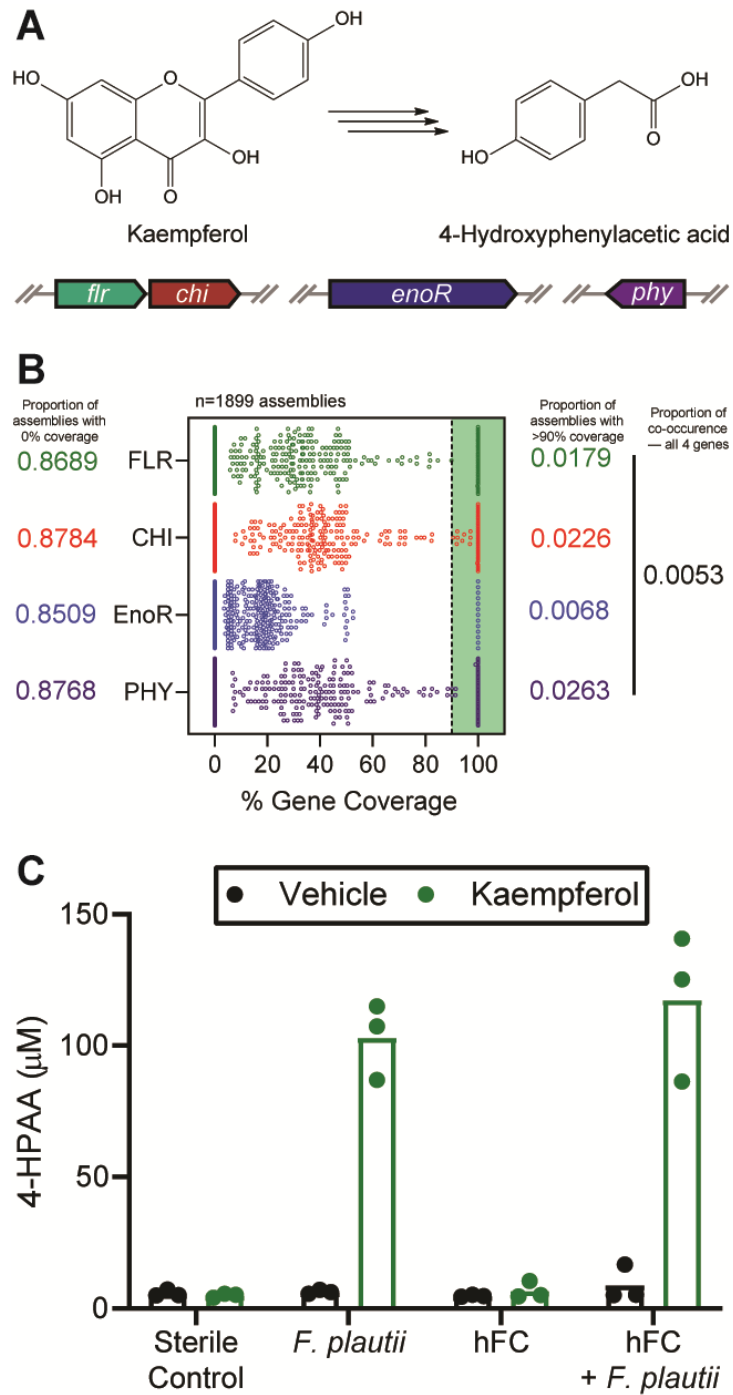


Fig. 4. 4-HPAA activates AMPK α and downstream effectors to reduce de novo hepatic lipogenesis. (A) Western blot analysis of pAMPK α (T172), total AMPK α , and β -actin with densitometric quantification, n=6 per group. (B) Western blot analysis of pACC (S79), total ACC, and β -actin with densitometric quantification, n=6 per group. (C) Primary murine hepatocytes were treated with either DMSO vehicle control (0 μ M) or 0.01, 0.1, 1, and 10 μ M 4-HPAA for 30 minutes at which point protein expression of pACC (S79), total ACC, pAMPK α (T172), total AMPK α , and β -actin were measured via Western blot analysis with densitometric quantification with dots representing the mean of two biological replicates. Statistical analysis for panels A and B was performed using unpaired two-tailed Student's t-test. Individual points represent individual mice, and bars represent group means.

599
600
601
602
603
604
605
606
607
608
609
610
611



612

613

614

615

616

617

618

619

620

621

Fig. 5. Flavonol and flavone catabolizing genes are rarely found in human microbiomes. (A) Graphical depiction of the complete bacterial gene set required to catabolize the flavonol kaempferol into 4-HPAA. (B) Computational screening of 1,899 assemblies of metagenomic data derived from human fecal samples representing over 1,300 human subjects for each of the bacterial genes required to catabolize flavonols/flavones. Assemblies with >90% coverage to the parent *Flavonifractor plautii* YL31 gene of interest were considered present. (C) *F. plautii* converts kaempferol into 4-HPAA after 24-hours of anaerobic incubation in vitro and retains its function when added to a non-converting human fecal community (hFC). Individual points represent individual technical replicates, and bars represent group means.